

Deprotonating Molecules and Free Radicals to Form Carbon-Centered Anions: A G2 ab Initio Study of Molecular and Free Radical Acidity

Paul M. Mayer^{1a,b} and Leo Radom^{*,1a}

Research School of Chemistry, Australian National University, Canberra, ACT 0200, Australia

Received: February 11, 1998

Molecules CH_3X and free radicals $\cdot\text{CH}_2\text{X}$ can be deprotonated to form carbon-centered anions CH_2X^- and radical anions $\text{HCX}^{\cdot-}$, respectively. We have studied the geometric and thermochemical changes that accompany such deprotonation processes for a variety of substituents X including the π -donor groups NH_2 , OH , OCH_3 , PH_2 , SH , F , Cl , and Br and the π -acceptor groups BH_2 , AlH_2 , CHO , NO_2 , CN , and NC . Thermochemical properties calculated and discussed include the gas-phase acidities of the molecules and free radicals, the electron affinities of the $\cdot\text{CH}_2\text{X}$ free radicals, various dissociation energies, and the heats of formation of all species. The acidities of $\cdot\text{CH}_2\text{X}$ radicals are predicted to be greater than those of CH_3X for π -donor substituents but less for π -acceptor substituents (except CN and NC). The changes that are predicted to occur upon deprotonation in C–X bond lengths, C–X homolytic and heterolytic bond dissociation enthalpies, C–H homolytic bond dissociation enthalpies, and radical stabilization energies may be understood by examining the orbital interactions that take place in each species.

Introduction

An important quantity pertaining to the deprotonation of a molecule in the gas phase is the enthalpy difference ($\Delta_{\text{acid}}H^\circ$) between a species (AH) and its deprotonation products ($\text{A}^- + \text{H}^+$):



The gas-phase acidities of molecules (hereafter simply referred to as acidities) have been experimentally determined with a variety of techniques ranging from kinetic studies using flowing-afterglow and selected-ion flow mass spectrometry, equilibrium measurements with high-pressure mass spectrometry, and bracketing experiments using FT-ICR mass spectrometry.² To complement experimental $\Delta_{\text{acid}}H^\circ$ data, ab initio molecular orbital calculations have been used to calculate the enthalpies of deprotonation of molecules.^{3,4} One of the most successful methods employed has been G2 theory,⁵ which has been found to generally predict acidities in good agreement with experimental values.⁴

A molecule such as CH_3YH can, in principle, be deprotonated at either the heteroatom or the carbon. The former process yields an anion centered on Y, while deprotonation of the methyl group leads to a carbon-centered anion. Typically, the heteroatom is the more acidic site (and is characterized by a lower $\Delta_{\text{acid}}H^\circ$; for example, the value for $\Delta_{\text{acid}}H^\circ$ corresponding to deprotonation of the methyl group in CH_3OH is 1735 kJ mol^{-1} (see text), while that for deprotonation of the hydroxy group is 1601 kJ mol^{-1}).⁴ The anion CH_2YH^- is nevertheless of interest, as it allows the effect of substituents on anion stability to be systematically studied by varying YH.

A free radical, $\cdot\text{CH}_2\text{YH}$, can also be deprotonated at either Y or C. Deprotonation at Y typically leads to the radical anion of a stable, closed-shell molecule (for example, deprotonation of the hydroxy group in $\cdot\text{CH}_2\text{OH}$ yields the radical anion of formaldehyde, $\text{CH}_2\text{O}^{\cdot-}$). These species are usually not very stable, the electron generally having a very small binding energy

or sometimes being unbound.⁶ Deprotonation at the radical center gives $\text{HCYH}^{\cdot-}$, the radical anion of a carbene. Carbenes may also have either positive electron affinities (yielding stable radical anions) or negative electron affinities (yielding thermodynamically unstable radical anions). However, regardless of whether the radical anion of a carbene is stable, studying $\text{HCYH}^{\cdot-}$ anions permits the investigation of the effect of substituents on the stability of radical anions.

The aim of the present work is to systematically study, at the G2 level of theory, the effect of deprotonation at carbon on the structure, stability, and thermochemistry of molecules and free radicals. We chose for this study a set of prototypical substituted methanes, CH_3X , and free radicals, $\cdot\text{CH}_2\text{X}$, where X represents a variety of substituents including the π -donor groups NH_2 , OH , OCH_3 , PH_2 , SH , F , Cl , and Br and the π -acceptor groups BH_2 and AlH_2 (σ -donors) and CHO , NO_2 , CN , and NC (σ -acceptors). The substituents thus include groups that are electropositive or electronegative with respect to carbon, as well as unsaturated groups that permit delocalization of electron density.

Computational Methods

Standard ab initio calculations⁷ were carried out using the GAUSSIAN 94⁸ and ACESII⁹ packages. Geometries were optimized at the MP2(full)/6-31G(d) level, and zero-point vibrational energies (ZPEs) (scaled by 0.8929) were obtained at the HF/6-31G(d) level in accordance with the G2 scheme.⁵ G2 theory effectively corresponds to a QCISD(T)/6-311+G-(3df,2p)/MP2(full)/6-31G(d) energy calculation, adjusted to 0 K by the zero-point vibrational energy, and includes an empirical higher-level correction (HLC) to account for residual basis set deficiencies.

Gas-phase acidities ($\Delta_{\text{acid}}H^\circ$) at 0 K were calculated as the enthalpy change for the deprotonation reaction 1. Since the HLC in G2 theory is the same for both the reactants and products in reaction 1, the G2 acidities are purely ab initio. Heats of

formation ($\Delta_f H^\circ$) at 0 K were calculated according to the atomization method outlined by Nicolaidis et al.¹⁰ Acidities and enthalpies of formation were corrected⁷ to 298 K with the use of the scaled HF/6-31G(d) vibrational frequencies for the species under consideration and experimental $H^\circ_{298} - H^\circ_0$ corrections for the elements in their standard state.¹¹

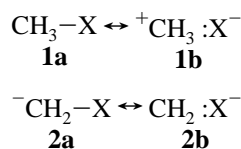
Unrestricted open-shell reference wave functions were used for all open-shell species. A potential problem in calculating the properties of open-shell systems is spin-contamination in the reference Hartree–Fock wave function. In a recent study,¹² we found that for free radicals exhibiting only moderate spin-contamination ($\langle S^2 \rangle \leq 0.8$), G2 theory can typically be expected to provide an adequate description of their thermochemistry. Most of the radicals and radical anions discussed in this paper fall into this category. However, for the few highly spin-contaminated species (HCBH₂^{•-}, HCAIH₂^{•-}, [•]CH₂CHO, [•]CH₂-CN, HCCN^{•-}, [•]CH₂NC, and HCNC^{•-}), the G2 results may be less accurate than normal. The G2 total energies of the substituted methanes, methyl radicals and their deprotonated counterparts at 298 K, along with values for $\langle S^2 \rangle$ for the radicals, can be found as Supporting Information (Table S1). The complete MP2(full)/6-31G(d) geometries for all species in this study are presented in the form of GAUSSIAN archive entries in Table S2 of the Supporting Information.

It has often been stated that the calculation of accurate geometries and energies of anions requires the incorporation of diffuse functions in the basis set.⁷ In a recent paper, Gronert³ examined the adequacy of the G2 computational scheme for small anions and explored the effect on the results of the addition of both a single and double set of diffuse functions. He concluded that for very small anions such as F⁻ and HO⁻, the striking quantitative success of G2 theory is mainly due to a fortuitous cancellation of errors. An alternative method was proposed (G2(DD)) corresponding to a G2 calculation in which (a) geometry optimizations are carried out at the MP2(full)/6-31+G(d) level and (b) single-point calculations are carried out with basis sets having two sets of diffuse functions. For his test set, Gronert found that the difference between theory and experiment for standard G2 theory was at most 8 kJ mol⁻¹ (for $\Delta_{\text{acid}}H^\circ$ of CH₄), the other discrepancies being less than 4 kJ mol⁻¹. The G2(DD) level of theory performed better, the maximum deviation being 4 kJ mol⁻¹. While recognizing the superior performance of G2(DD), we did not believe that the extra computational costs of using G2(DD) rather than G2 were warranted in the present study, especially as the species in the present work are much larger than the problem cases discussed by Gronert (and may therefore be better behaved).¹³

Results and Discussion

It is useful to begin by considering in qualitative terms the effects of deprotonation on the bonding in CH₃X and [•]CH₂X. This then forms a basis for understanding our quantitative structural and thermochemical results.

1. Effects of Deprotonation on CH₃X. A molecule CH₃X or anion CH₂X⁻ can be described as having two resonance contributors, a single-bond (covalent) structure (**a**) and a no-bond (ionic) structure (**b**):



In a neutral species CH₃X, the electron affinity (EA) of X (Table

TABLE 1: Comparison of Calculated and Experimental Electron Affinities of CH₂, CH, and Substituents X^a

species	G2 ^b	experiment ^c
CH ₂	0.66	0.652 ± 0.006
CH	1.13	1.238 ± 0.008
NH ₂	0.77	0.75 ± 0.06
OH	1.87	1.828
OCH ₃	1.62	1.62 ± 0.14
PH ₂	1.25	1.6
SH	2.30	2.32 ± 0.10
F	3.48	3.399 ± 0.003
Cl	3.60	3.617 ± 0.003
Br	3.10	3.365 ± 0.003
BH ₂	0.34	
AlH ₂	1.15	
CHO	0.34	0.313 ± 0.005
NO ₂	2.34	2.30 ± 0.10
CN	3.97	3.74 ± 0.17

^a EA values in eV at 0 K. ^b Some of these values may also be found in Curtiss et al.^{5a} ^c Lias et al.¹⁴

1) is typically much smaller than the IE of CH₃ (9.84 eV),¹⁴ and thus the bonded resonance structure **1a** dominates the description of the C–X bond. When CH₃X is deprotonated at carbon to produce CH₂X⁻, the EA of X is generally greater than the EA of CH₂ (Table 1), and thus the no-bond structure **2b** begins to become more significant in describing the C–X bond. This is in some ways similar to what happens when a CH₃X molecule is protonated: the C–X bond in CH₃XH⁺ takes on ⁺C:XH character, this character increasing with increasing ionization energy of XH.^{15,16} In the case of the anions, the importance of the no-bond structure will increase as the EA of X increases, being most prominent for the halogens and least prominent for the groups BH₂, NH₂, and CHO (see Table 1).

There will be additional conjugative and hyperconjugative interactions in the neutral and deprotonated species that may act in the same or opposite direction to the effects resulting from no-bond resonance contributions.

When X is a π -donor substituent (X = NH₂, OH, OCH₃, PH₂, SH, F, Cl, or Br), hyperconjugative electron donation in CH₃X can take place from a lone pair on X (n(X)) to a pseudo- π^* -orbital of the methyl group ($\pi^*(\text{CH}_3)$).^{16,17} When X is a π -acceptor, σ -donor group (BH₂ or AlH₂), hyperconjugative electron donation can take place from a pseudo- π -orbital on CH₃ ($\pi(\text{CH}_3)$) to the vacant p-orbital on the heteroatom in CH₃X, 2p(X). For X = CHO, NO₂, CN, and NC (π -acceptor, σ -donor groups), hyperconjugative donation occurs from $\pi(\text{CH}_3)$ to $\pi^*(\text{X})$ in CH₃X.

For π -donor substituents X, the preferred structure of CH₂X⁻ attempts to minimize the unfavorable four-electron interaction between the lone pair on C with the lone pair on X through appropriate rotation about the C–X bond (Figure 1). Intriguingly, the observation that the C–H bonds in the anions are lengthened relative to those in CH₃X and the N–H and O–H bonds are relatively unchanged (see Supporting Information) suggests a weak n(X) → $\pi^*(\text{CH}_2)$ interaction for the NH₂ and OH substituents. For second-row substituents such as PH₂, this donation appears to be reversed, resulting in a two-electron donation from n(C⁻) to $\pi^*(\text{PH}_2)$ (lengthening the P–H bonds relative to CH₃X, while leaving the C–H bonds relatively unchanged).

When X is a π -acceptor, σ -donor group (BH₂ or AlH₂), there is a favorable two-electron interaction in CH₂X⁻ between the lone pair on carbon, n(C⁻), and the vacant 2p(X) orbital on the heteroatom (Figure 1). The ⁻CH₂X anions with the π -acceptor, σ -acceptor substituents X = CHO, NO₂, CN, and NC exhibit a similar donation to $\pi^*(\text{X})$.

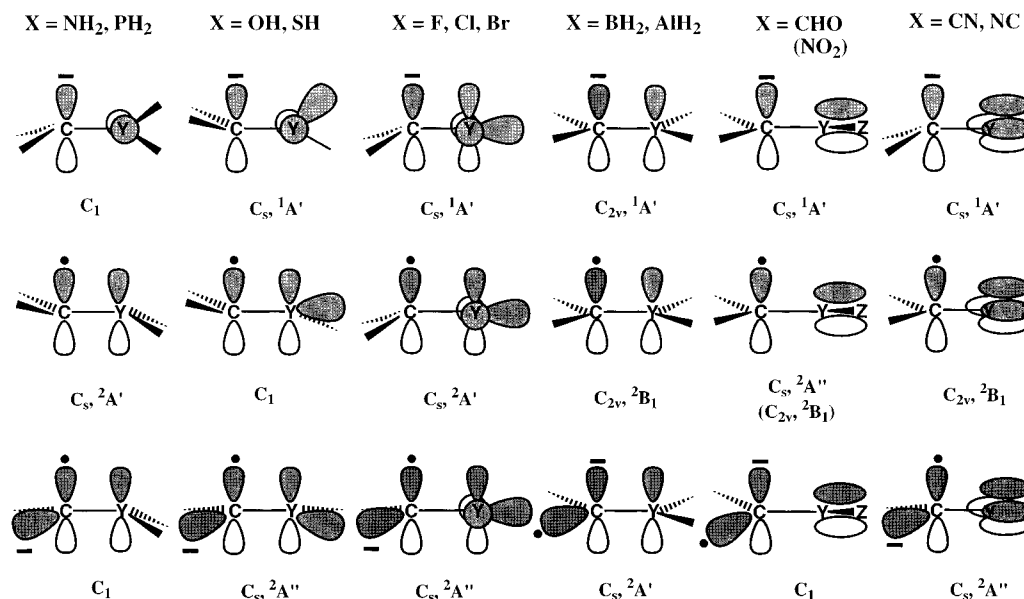
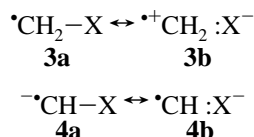


Figure 1. Schematic orbital diagrams for the CH_2X^- anions, $\cdot\text{CH}_2\text{X}$ radicals, and HCX^- radical anions.

2. Effects of Deprotonation on $\cdot\text{CH}_2\text{X}$. Like the closed-shell species, the bonding in $\cdot\text{CH}_2\text{X}$ radicals and HCX^- radical anions can be described by two resonance structures:



The degree to which **3b** and **4b** participate is a function of the relative values of the electron affinity of X and the ionization energies of CH_2 and CH^- (Table 1), being greatest for substituents X with large EA values.

There are additional orbital interactions in both the neutral and anionic free radicals. The radicals $\cdot\text{CH}_2\text{X}$ with π -donor groups are stabilized by a three-electron interaction between $p(\text{C})$ and $n(\text{X})$.^{16,17} When X = BH_2 or AlH_2 , the formally singly occupied orbital on carbon, $p(\text{C})$, can be delocalized to the vacant $2p(\text{X})$ orbital on the heteroatom. The other π -acceptor groups also allow delocalization of the unpaired electron.

The three-electron interaction between $p(\text{C})$ and $n(\text{X})$ in HCX^- (when X is a π -donor group) is less favorable than it is in the neutral radicals $\cdot\text{CH}_2\text{X}$ since it would result in an increase in electron density at an already formally negatively charged carbon atom. When X is BH_2 or AlH_2 , the $^2\text{A}'$ ground state allows favorable two-electron donation from the lone pair on C, $n(\text{C}^-)$, to $2p(\text{X})$ in HCX^- . The unpaired electron in these radical anions resides in an orbital that lies in the molecular plane (Figure 1). A similar situation exists when X = CHO and NO_2 , with delocalization of the lone pair on carbon taking place to the π -system of X. However, unlike the situation for the HCX^- radical anions with the other π -acceptor groups, HCCN^- and HCNC^- have a $^2\text{A}''$ ground state in which the orbital containing the unpaired electron, rather than the lone pair, is orthogonal to the molecular plane (Figure 1). We have investigated the $^2\text{A}'$ state of HCCN^- (which would allow maximum delocalization of the lone pair to CN) and found it to lie 70 kJ mol^{-1} higher in energy than the ground $^2\text{A}''$ state (at the G2 level of theory).

3. Effects of Deprotonation on the C–X Bond Lengths in CH_3X and $\cdot\text{CH}_2\text{X}$. The C–X bond lengths in CH_3X , CH_2X^- , $\cdot\text{CH}_2\text{X}$, and HCX^- are listed in Table 2. For the

TABLE 2: C–X Bond Lengths^a in Substituted Methanes, Methyl Radicals, and Their Deprotonated Forms

X	$r(\text{C}-\text{X})$			
	CH_3X	CH_2X^-	$\cdot\text{CH}_2\text{X}$	HCX^-
NH ₂	1.465	1.520	1.402	1.516
OH	1.424	1.544	1.373	1.522
OCH ₃	1.414	1.504	1.363	1.498
PH ₂	1.860	1.739	1.807	1.773
SH	1.816	1.805	1.728	1.856
F	1.390	1.516	1.350	1.498
Cl	1.779	1.960	1.718	1.960
Br	1.949	2.135	1.863	2.136
BH ₂	1.561	1.451	1.530	1.411
AlH ₂	1.961	1.848	1.930	1.802
CHO	1.502	1.380	1.456	1.393
NO ₂	1.486	1.352	1.431	1.404
CN	1.461	1.398	1.412	1.405
NC	1.423	1.411	1.360	1.411

^a Bond lengths in Å.

π -donor groups, the C–X bonds in CH_2X^- are generally longer than in CH_3X due to an increased contribution of the no-bond resonance structure **2b**. A notable exception is the PH_2 substituent, where it appears that the competing $n(\text{C}^-) \rightarrow \pi^*$ -(PH_2) interaction leads to an overall shortening of the C–X bond.

The C–X bond becomes shorter upon deprotonation of CH_3X when X is a π -acceptor substituent due to the interaction of the lone pair on C with the π -acceptor orbital on X, as outlined in section 1.

The HCX^- radical anions generally exhibit longer C–X bonds than $\cdot\text{CH}_2\text{X}$ when X is a π -donor substituent. This may also be attributed to the enhanced contribution of the no-bond resonance structure **4b** and the diminished $n(\text{X}) \rightarrow p(\text{C})$ interaction. The C–X bond in HCPH_2^- is shorter than in $\cdot\text{CH}_2\text{-PH}_2$, as was also observed for the $\text{CH}_2\text{PH}_2^-/\text{CH}_3\text{PH}_2$ pair. When X = SH and Cl, however, the high EAs of SH and Cl mean that **4b** dominates the description of the C–X bond, resulting in longer C–X bonds in HCSH^- and HCCl^- than in $\cdot\text{CH}_2\text{SH}$ and $\cdot\text{CH}_2\text{Cl}$.

The HCX^- anions with π -acceptor groups exhibit shorter C–X bonds than in the $\cdot\text{CH}_2\text{X}$ free radicals (except for X = NC). For BH_2 , AlH_2 , CHO, and NO_2 , this is due to the

TABLE 3: Calculated Homolytic and Heterolytic BDEs for Substituted Methanes, Methyl Radicals, and Their C-Deprotonated Counterparts^a

	homolytic BDE		heterolytic BDE	
	C–X	[•] C–X	C–X	[•] C–X
CH ₃ –NH ₂	358.2	322.2	1226.4	311.4
[•] CH ₂ –NH ₂	429.8	321.4	1350.3	355.6
CH ₃ –OH	391.6	373.1	1153.5	256.1
[•] CH ₂ –OH	450.2	377.9	1264.4	306.0
CH ₃ –OCH ₃	359.3	348.4	1145.4	255.4
[•] CH ₂ –OCH ₃	418.4	344.3	1256.7	296.4
CH ₃ –PH ₂	302.3	370.6	1124.7	314.0
[•] CH ₂ –PH ₂	352.7	336.2	1227.4	324.7
CH ₃ –SH	313.5	366.3	1034.1	207.9
[•] CH ₂ –SH	376.3	356.4	1149.2	243.1
CH ₃ –F	470.1	469.2	1077.3	197.5
[•] CH ₂ –F	507.6	469.9	1167.1	243.2
CH ₃ –Cl	353.6	405.0	948.8	121.2
[•] CH ₂ –Cl	399.1	396.5	1046.6	157.7
CH ₃ –Br	292.8	362.8	936.7	127.8
[•] CH ₂ –Br	333.1	352.6	1029.3	162.6
CH ₃ –BH ₂	444.1	641.8	1354.4	673.1
[•] CH ₂ –BH ₂	511.1	562.0	1473.7	638.3
CH ₃ –AlH ₂	350.2	497.9	1182.2	450.9
[•] CH ₂ –AlH ₂	403.0	432.5	1287.3	430.5
CH ₃ –CHO	357.0	536.3	1267.2	567.4
[•] CH ₂ –CHO	418.5	438.1	1380.9	514.3
CH ₃ –NO ₂	263.6	480.4	980.2	317.9
[•] CH ₂ –NO ₂	300.4	394.0	1069.2	276.6
CH ₃ –CN	520.3	667.4	1079.6	347.8
[•] CH ₂ –CN	578.0	643.8	1189.7	369.2
CH ₃ –NC	421.3	532.8	980.7	213.2
[•] CH ₂ –NC	482.2	528.8	1093.8	254.2

^a In kJ mol⁻¹ at 298 K.

delocalization of the lone pair to X. Although, as noted above, the preferred geometric structure of HCCN^{•-} does not allow an optimum interaction of this type, delocalization of the lone pair may still take place to the second π*-orbital (Figure 1). The interaction is reduced when X = NC, perhaps due to the partial negative charge on the terminal carbon of the isocyanato group.

4. Effects of Deprotonation on the C–X Bond Dissociation Enthalpies in CH₃X and [•]CH₂X. The heterolytic and homolytic C–X bond dissociation enthalpies for CH₃X, CH₂X⁻, [•]CH₂X and HCX^{•-} are listed in Table 3.

The most striking observation in Table 3 is the dramatic drop in the heterolytic BDEs in the anions relative to the neutrals. The reductions in heterolytic BDEs follow the trend in the electron affinities of X (Table 1). As the EA of X increases, the contributions from the no-bond resonance structures **2b** and **4b** will also increase, facilitating heterolytic cleavage.

The homolytic BDEs do not follow the same pattern as the heterolytic BDEs. The CH₂X⁻ anions with first-row π-donor substituents (X = NH₂, OH, OCH₃, or F) have smaller homolytic BDEs than their CH₃X counterparts. The four-electron repulsion between n(C⁻) and n(X) weakens the C–X bonds in these cases. The anions with the second- and third-row π-donor substituents (X = PH₂, SH, Cl, or Br) all have stronger homolytic BDEs than their CH₃X analogues.

The CH₂X⁻ anions with π-acceptor substituents all display larger C–X homolytic BDEs than CH₃X. This is due to the favorable interaction between the lone pair on C and 2p(X) (for BH₂ and AlH₂) or π(X) and π*(X) (for X = CHO, NO₂, CN, and NC).

The [•]CH₂X radicals with π-donor groups (except for Br) exhibit a decrease in homolytic BDE upon deprotonation (Table 3) due to the reduction in the n(X) → p(C) interaction in HCX^{•-},

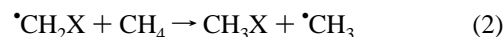
TABLE 4: Calculated Stabilization Energies for [•]CH₂X and HCX^{•-} and Homolytic C–H Bond Dissociation Enthalpies for CH₃X and CH₂X⁻

X	RSE ^a	RASE ^b	C–H BDE ^c	
	[•] CH ₂ X	HCX ^{•-}	CH ₃ X	CH ₂ X ⁻
H	0	0	442.6	408.4
NH ₂	+46.9	+37.0	395.7	371.3
OH	+33.9	+42.6	408.7	365.7
OCH ₃	+34.1	+33.7	408.5	374.7
PH ₂	+25.6	+3.5	417.0	404.9
SH	+38.1	+27.9	404.5	380.4
F	+12.7	+38.5	429.9	369.9
Cl	+20.7	+29.3	421.9	379.1
Br	+15.5	+27.6	427.0	380.7
BH ₂	+42.2	-42.0	400.3	450.4
AlH ₂	+28.0	-27.7	414.5	436.0
CHO	+36.7	-60.4	405.9	468.7
NO ₂	+12.0	-48.6	430.6	456.9
CN	+33.0	+14.2	409.6	394.2
NC	+36.1	+33.8	406.5	374.6

^a Enthalpy change for the reaction [•]CH₂X + CH₄ → CH₃X + [•]CH₃, in kJ mol⁻¹ at 298 K. ^b Enthalpy change for the reaction HCX^{•-} + CH₃⁻ → CH₂X⁻ + CH₂^{•-}, in kJ mol⁻¹ at 298 K. ^c Enthalpy change for the reactions CH₃X → [•]CH₂X + H[•] and CH₂X⁻ → HCX^{•-} + H[•], respectively, in kJ mol⁻¹ at 298 K.

as noted above. As was observed for the closed-shell species, there is an increase in homolytic BDE in HCX^{•-} relative to [•]CH₂X when X is a π-acceptor substituent.

5. Effect of Deprotonation on the Radical Stabilization Energies of [•]CH₂X. There have been many publications dealing with the question of free radical stability, and many of the factors that influence the stability of radicals have been discussed in detail.^{16,18} The radical stabilization energies (RSEs) for substituted methyl radicals may be defined as the calculated enthalpy changes for reaction 2 (Table 4):



while the radical anion stabilization energies (RASEs) for their deprotonated forms, the substituted methylene radical anions, may be defined as the enthalpy changes in reaction 3 (Table 4):



The RSEs for π-donor and π-acceptor substituents have been discussed in detail in a previous publication.¹⁶ Briefly, the [•]CH₂X radicals with π-donor groups such as NH₂ are stabilized by the n(X) → p(C) interaction, while the radicals with π-acceptor groups such as BH₂ or CN are stabilized by delocalization of the unpaired electron to X.

The π-donor groups all stabilize HCX^{•-} relative to CH₂X⁻, due to the n(X) → p(C) interaction in the radical anions, which is absent in the closed-shell anions. The RASE values of the radical anions substituted by BH₂, AlH₂, CHO, or NO₂ groups are negative; that is, the HCX^{•-} radical anions are destabilized relative to CH₂X⁻, while CN and NC both are found to stabilize the radical anions.

The stabilization energies defined by reactions 2 and 3 correspond to values of C–H bond dissociation enthalpies for CH₃X and CH₂X⁻ relative to CH₄ and CH₃⁻, respectively. For completeness, the absolute values of the C–H BDEs in CH₃X and CH₂X⁻ are also included in Table 4.

6. Gas-Phase Acidities (Δ_{acid}H^o) of Molecules CH₃X and Free Radicals [•]CH₂X. The G₂ values of Δ_{acid}H^o for CH₃X and [•]CH₂X are listed in Table 5 along with values from the

TABLE 5: Comparison of Calculated and Experimental C-Centered Gas-Phase Acidities^a

species	G2 $\Delta_{\text{acid}}H^{\circ}$	literature $\Delta_{\text{acid}}H^{\circ}$ values	
		experiment	theory ^b
CH ₃ NH ₂	1752.3		1754.9, ^c 1755 ^d
•CH ₂ NH ₂	1727.9		
CH ₃ OH	1734.7		1730.1, ^c 1736.3 ^d
•CH ₂ OH	1691.8		
CH ₃ OCH ₃	1727.3	1703 ± 8 ^e	
•CH ₂ OCH ₃	1693.6		
CH ₃ PH ₂	1648.1		1663.8 ^c
•CH ₂ PH ₂	1636.0		
CH ₃ SH	1663.5		1671.4, ^c 1675.2 ^d
•CH ₂ SH	1639.4		
CH ₃ F	1717.2		1709.4, ^c 1718, ^f 1720.4 ^g
•CH ₂ F	1657.2	1668 ± 16 ^b	1657 ^f
CH ₃ Cl	1666.0	1657 ± 15 ^e	1675.7, ^c 1667 ^f
•CH ₂ Cl	1622.2	1610 ± 10 ^b	1630 ^f
CH ₃ Br	1646.3	1643 ± 16 ^e	1645.5 ^c
•CH ₂ Br	1600.0	1593 ± 8 ^b	
CH ₃ BH ₂	1518.6		1524.8 ^c
•CH ₂ BH ₂	1568.7		
CH ₃ AlH ₂	1568.7		1564 ^c
•CH ₂ AlH ₂	1590.1		
CH ₃ CHO	1540.1	1531 ± 12, ^e 1533 ± 12 ^e	
•CH ₂ CHO	1599.9		
CH ₃ NO ₂	1499.6	1491 ± 12 ^e	
•CH ₂ NO ₂	1525.9		
CH ₃ CN	1569.2	1560 ± 11, ^e 1559 ± 13 ⁱ	1605.2, ^g 1574, ^j 1567.2 ^k
•CH ₂ CN	1553.7	1569 ± 18, ^e 1563 ± 3 ⁱ	
CH ₃ NC	1604.8	1589 ± 8 ⁱ	1605.7 ^k
•CH ₂ NC	1572.9	1582 ± 10 ⁱ	

^a In kJ mol⁻¹ at 298 K. Some of the G2 values have also been quoted by Smith and Radom.⁴ ^b If 0 K values were reported, they have been corrected to 298 K using the thermal correction factors obtained in the present study. ^c El-Nahas et al.^{19b} ^d Downard et al.^{3c} ^e Lias et al.¹⁴ ^f Rodriguez et al.^{3e} ^g Edgecombe et al.^{3a} ^h Born et al.^{20b} ⁱ Matimba et al.^{20a} ^j Jorgensen et al.^{19a} ^k Wiberg et al.^{3h}

literature.^{3a,c,e,h,4,14,19,20} There is a paucity of experimental data available for carbon-centered acidities of molecules, partly because deprotonation of CH₃X generally occurs preferentially at the heteroatom (as in CH₃OH, see above). The experimental data that are available are thus almost exclusively for systems bearing substituents that do not contain hydrogen (F, CN, etc.). Experimental determination of the carbon-centered acidities of radicals is a more difficult problem, but Nibbering and co-workers²⁰ have measured the acidities of the halo-, cyano-, and isocyano-substituted free radicals using the bracketing method and FT-ICR mass spectrometry. Our calculated acidities are generally in good agreement with the quoted experimental data for both molecules and free radicals.

The relative acidities of CH₃X and •CH₂X reflect the relative stabilities of CH₂X⁻ and HCX^{•-}: the greater the stability of the anions, the greater the acidity (and the smaller the $\Delta_{\text{acid}}H^{\circ}_{298}$ value). For the π -donor groups (X = NH₂, OH, OCH₃, PH₂, SH, F, Cl, and Br), the •CH₂X radicals exhibit smaller $\Delta_{\text{acid}}H^{\circ}_{298}$ values relative to CH₃X, reflecting the greater relative stability of HCX^{•-} in these cases (see section 5). This is also the case for CN- and NC-substituted radicals. The $\Delta_{\text{acid}}H^{\circ}_{298}$ values for the free radicals with the other π -acceptor substituents (X = BH₂, AlH₂, CHO, and NO₂) are larger than for their CH₃X counterparts due to the destabilization of the resultant radical anions.

7. Heats of Formation of CH₃X, CH₂X⁻, •CH₂X, and HCX^{•-}. The heats of formation at 298 K for all of the species discussed in this paper can be found in Table 6, where they are compared with recent experimental and theoretical values.^{3f,14,20,21} The comparison of the calculated and experimental values for many of the closed-shell neutral molecules and neutral free

TABLE 6: Comparison of Calculated and Experimental Heats of Formation^a

species	G2 $\Delta_f H^{\circ}_{298}$	experimental $\Delta_f H^{\circ}_{298}$	
		Lias et al. ^b	other data
CH ₃ NH ₂	-22.8	-23.0 ± 0.4	
CH ₂ NH ₂ ⁻	198.7		
•CH ₂ NH ₂	154.8	159 ± 8	150.6 ^c
HCNH ₂ ^{•-}	352.1		
CH ₃ OH	-206.7	-201.6 ± 0.2	
CH ₂ OH ⁻	-2.7		
•CH ₂ OH	-16.0	-26 ± 6	-16.6 ± 0.9, ^d -16.6 ± 1.3 ^e
HCOH ^{•-}	145.0		
CH ₃ OCH ₃	-192.4	-184.0 ± 0.5	f
CH ₂ OCH ₃ ⁻	4.2	-11 ± 9	
•CH ₂ OCH ₃	-2.0	-13 ± 4	-5.4 ± 8 ^{g,f}
HCOCH ₃ ^{•-}	160.8		
CH ₃ PH ₂	-19.4	-18	
CH ₂ PH ₂ ⁻	98.0		
•CH ₂ PH ₂	179.6		
HCPH ₂ ^{•-}	284.8		
CH ₃ SH	-20.5	-22.9 ± 0.6	
CH ₂ SH ⁻	112.3		
•CH ₂ SH	166.1		150.0 ± 8.4 ^h
HCSH ^{•-}	274.7		
CH ₃ F	-244.4	-247	i
CH ₂ F ⁻	-58.0		
•CH ₂ F	-32.6	-33 ± 8	-31.8 ± 8.4 ^j
HCF ^{•-}	93.9	< 116	106 ^{k,l}
CH ₃ Cl	-85.5	-82.0 ± 0.5	
CH ₂ Cl ⁻	48.7	45 ± 16	
•CH ₂ Cl	118.4	130	117.3 ± 3.1, ^m 116 ± 8 ⁿ
HCCl ^{•-}	209.8		197 ^{k,l}
CH ₃ Br	-34.0	-38.1 ± 1.3	
CH ₂ Br ⁻	81.6	75 ± 18	
•CH ₂ Br	175.1	174	168 ± 8 ⁿ
HCB ^{•-}	244.3		237 ^o
CH ₃ BH ₂	22.9		
CH ₂ BH ₂ ⁻	10.9		
•CH ₂ BH ₂	205.3		
HCBH ₂ ^{•-}	243.2		
CH ₃ AlH ₂	56.4		
CH ₂ AlH ₂ ⁻	94.3		
•CH ₂ AlH ₂	252.9		
HCAIH ₂ ^{•-}	312.3		
CH ₃ CHO	-174.3	-165.8 ± 0.4	
CH ₂ CHO ⁻	-164.9	-165 ± 13	
•CH ₂ CHO	16.6		
HCCHO ^{•-}	85.8		
CH ₃ NO ₂	-86.7	-74.8 ± 1.0	
CH ₂ NO ₂ ⁻	-117.8	-114 ± 13	
•CH ₂ NO ₂	125.9		
HCNO ₂ ^{•-}	121.1	< 59	
CH ₃ CN	75.7	74 ± 1	
CH ₂ CN ⁻	114.1	105 ± 12, 20 ± 19	101 ± 8 ^p
•CH ₂ CN	267.2	245 ± 10	243 ± 13, ^q 250 ± 8 ^p
HCCN ^{•-}	290.3	< 422, 309 ± 19	287 ± 11 ^p
CH ₃ NC	174.6	173 ± 1	
CH ₂ NC ⁻	248.7		232 ± 8 ^p
•CH ₂ NC	363.1		402 ± 13, ^q 334 ± 8 ^p
HCNC ^{•-}	405.3		386 ± 18 ^p

^a In kJ mol⁻¹ at 298 K. ^b Lias et al.¹⁴ ^c Griller and Lossing.^{21a} ^d Ruscic and Berkowitz.^{21b} ^e Dóbbé et al.^{21c} ^f G2 value of -184.1 kJ mol⁻¹ for CH₃OCH₃ and +3.8 kJ mol⁻¹ for •CH₂OCH₃ using isodesmic reactions (Good and Francisco).^{21d} ^g Holmes and Lossing.^{21e} ^h Ruscic and Berkowitz.^{21f} ⁱ Theoretical value of -240 ± 5 kJ mol⁻¹ by Espinosa-Garcia.^{21g} ^j Pickard and Rodgers.^{21h} ^k Using $\Delta_{\text{acid}}H^{\circ}_{298}$ and $\Delta_f H^{\circ}_{298}$ values for •CH₂X from Born et al.^{20b} and this table, respectively. ^l Theoretical value of 94.1 kJ mol⁻¹ by Rodriguez et al.^{3f} ^m Seetula.²¹ⁱ ⁿ Holmes and Lossing.^{21j} ^o Theoretical value of 210.9 kJ mol⁻¹ by Rodriguez et al.^{3f} ^p Matimba et al.^{20a} ^q Holmes et al.^{21k}

radicals has been discussed in a previous publication.¹⁶ Agreement with the values listed by Lias et al.¹⁴ is generally fairly good and becomes better when more recent experimental values for the free radicals are considered (Table 6). Experimental values for the carbon-centered anions are less readily available.

TABLE 7: Comparison of Calculated and Experimental Electron Affinities of $\cdot\text{CH}_2\text{X}$ Radicals^a

X	G2	experiment
NH ₂	-0.46	
OH	-0.14	
OCH ₃	-0.07	
PH ₂	0.84	
SH	0.55	
F	0.26	
Cl	0.73	0.80 ± 0.24 ^b
Br	0.97 ^c	1.0 ± 0.3 ^b
BH ₂	2.01	
AlH ₂	1.64	
CHO	1.88	1.817 ± 0.023 ^b
NO ₂	2.51	<2.36 ^b
CN	1.58	1.54 ± 0.01 ^d
NC	1.17	1.06 ± 0.02 ^e

^a In eV at 0 K. ^b Lias et al.¹⁴ ^c See also Ma et al.^{22a} ^d Moran et al.^{22b} ^e Moran et al.^{22c}

The G2 values for the radical anions compare favorably with those obtained by combining the recent acidity values for the free radicals of Nibbering and co-workers²⁰ with the experimental $\Delta_f H^\circ_{298}$ values for the free radicals in Table 6.

8. Electron Affinities of $\cdot\text{CH}_2\text{X}$. Table 7 lists the EAs of the $\cdot\text{CH}_2\text{X}$ radicals discussed in this study. In general, agreement between the calculated G2 values and the available experimental data^{14,22} is good. The radicals with the highest EAs are $\cdot\text{CH}_2\text{NO}_2$, $\cdot\text{CH}_2\text{BH}_2$, $\cdot\text{CH}_2\text{CHO}$, $\cdot\text{CH}_2\text{AlH}_2$, $\cdot\text{CH}_2\text{CN}$, and $\cdot\text{CH}_2\text{NC}$, i.e., those containing π -acceptor substituents. The high EAs reflect the increased stabilities of the CH_2X^- anions. The electron affinities of the $\cdot\text{CH}_2\text{X}$ radicals with X = NH₂, OH, and OCH₃ are negative, while the radicals with second-row π -donor X groups have small positive EAs.

Conclusions

Several significant conclusions can be drawn from this study.

(a) Deprotonation at carbon in CH_3X and $\cdot\text{CH}_2\text{X}$ leads to the CH_2X^- and HCX^- anions, respectively, and an increase in the contribution of the no-bond resonance structure to the description of the C–X bond with an associated large decrease in the C–X heterolytic BDE. The C–X bonds are shortened and (homolytically) strengthened when X is a π -acceptor such as BH₂ or CN, while for π -donor groups the bonds are lengthened and weakened as the EA of X increases.

(b) The HCX^- radical anions are stabilized relative to CH_2X^- for π -donor substituents but destabilized for π -acceptor substituents, except for CN and NC.

(c) The relative gas-phase acidities of CH_3X versus $\cdot\text{CH}_2\text{X}$ largely reflect the relative stabilities of CH_2X^- and HCX^- : $\cdot\text{CH}_2\text{X}$ is more acidic than CH_3X (i.e., smaller $\Delta_{\text{acid}}H^\circ_{298}$) when HCX^- is stabilized relative to CH_2X^- . Thus, $\Delta_{\text{acid}}H^\circ_{298}$ values are smaller for $\cdot\text{CH}_2\text{X}$ than CH_3X for π -donor substituents and larger for $\cdot\text{CH}_2\text{X}$ than CH_3X for π -acceptor substituents except for CN and NC.

(d) The geometrical and thermochemical changes that accompany deprotonation of CH_3X and $\cdot\text{CH}_2\text{X}$ can be rationalized to a large extent using orbital interaction arguments.

Acknowledgment. We thank Professor Nico Nibbering for helpful discussions and acknowledge a generous allotment of computer time on the Fujitsu VPP300 and SGI PowerChallenge computers at the Australian National University Supercomputing Facility.

Supporting Information Available: Total G2 energies at 298 K and values of $\langle S^2 \rangle$ (Table S1), GAUSSIAN archive entries

for the MP2(full)/6-31G(d) optimized geometries (Table S2), and the geometric and energetic effects of optimizing the HCF^- and HCCN^- radical anions with a basis set incorporating a set of diffuse functions (Table S3) (11 pages). See any current masthead page for ordering and Internet access instructions.

References and Notes

- (1) (a) Australian National University. (b) Present address: Chemistry Department, University of Ottawa, Ottawa, Canada K1N 6N5.
- (2) For a review of methods for determining $\Delta_{\text{acid}}H^\circ$, see: Berkowitz, J.; Ellison, G. B.; Gutman, D. *J. Phys. Chem.* **1994**, *98*, 2744.
- (3) (a) Edgecombe, J. E.; Boyd, R. J. *Can. J. Chem.* **1984**, *62*, 2887. (b) Schleyer, P. v. R.; Spitznagel, G. W.; Chandrasekhar, J. *Tetrahedron Lett.* **1986**, *27*, 4411. (c) Downard, K. M.; Sheldon, J. C.; Bowie, J. H.; Lewis, D. E.; Hayes, R. N. *J. Am. Chem. Soc.* **1989**, *111*, 8112. (d) Ritchie, J. P.; Bachrach, S. M. *J. Am. Chem. Soc.* **1990**, *112*, 6514. (e) Rodriguez, C. F.; Sirois, S.; Hopkinson, A. C. *J. Org. Chem.* **1992**, *57*, 4869. (f) Rodriguez, C. F.; Hopkinson, A. C. *J. Phys. Chem.* **1993**, *97*, 849. (g) Rodriguez, C. F.; Hopkinson, A. C. *J. Mol. Struct. (THEOCHEM)* **1993**, *280*, 205. (h) Wiberg, K. B.; Castejon, H. *J. Org. Chem.* **1995**, *60*, 6327. (i) Merrill, G. N.; Kass, S. R. *J. Phys. Chem.* **1996**, *100*, 17465. (j) Gronert, S. *Chem. Phys. Lett.* **1996**, *252*, 415.
- (4) For a detailed study of G2 predictions of gas-phase acidities, see: Smith, B. J.; Radom, L. *J. Phys. Chem.* **1991**, *95*, 10549.
- (5) (a) Curtiss, L. A.; Raghavachari, K.; Trucks, G. W.; Pople, J. A. *J. Chem. Phys.* **1991**, *94*, 7221. (b) Curtiss, L. A.; McGrath, M. P.; Blaudau, J.-P.; Davis, N. E.; Binning, R. C., Jr.; Radom, L. *J. Chem. Phys.* **1995**, *103*, 6104. For reviews of the applications of G2 theory, see: (c) Curtiss, L. A.; Raghavachari, K. In *Quantum Mechanical Electronic Structure Calculations with Chemical Accuracy*; Langhoff, S. R., Ed.; Kluwer Academic Press: Netherlands, 1995. (d) Raghavachari, K.; Curtiss, L. A. In *Modern Electronic Structure Theory*; Yarkony, D. R., Ed.; World Scientific: Singapore, 1995.
- (6) The EA of formaldehyde is negative, unpublished data.
- (7) Hehre, W. J.; Radom, L.; Schleyer, P. v. R.; Pople, J. A. *Ab Initio Molecular Orbital Theory*; Wiley: New York, 1986.
- (8) Frisch, M. J.; Trucks, G. W.; Schlegel, H. B.; Gill, P. M. W.; Johnson, B. G.; Robb, M. A.; Cheesman, J. R.; Keith, T.; Petersson, A.; Montgomery, A.; Raghavachari, K.; Al-Laham, M. A.; Zakrzewski, V. G.; Ortiz, J. V.; Foresman, J. B.; Cioslowski, J.; Stefanov, B. B.; Nanayakkara, A.; Challacombe, M.; Peng, C. Y.; Ayala, P. Y.; Chen, W.; Wong, M. W.; Andres, J. L.; Replogle, E. S.; Gomperts, R.; Martin, R. L.; Fox, D. J.; Binkley, J. S.; Defrees, D. J.; Baker, J.; Stewart, J. P.; Head-Gordon, M.; Gonzalez, C.; Pople, J. A. *GAUSSIAN 94*; Gaussian, Inc.: Pittsburgh, PA, 1995.
- (9) (a) Stanton, J. F.; Gauss, J.; Watts, J. D.; Lauderdale, W. J.; Bartlett, R. J. In *Quantum Theory Project, Departments of Chemistry and Physics, University of Florida: Gainesville, 1992*. (b) Stanton, J. F.; Gauss, J.; Watts, J. D.; Lauderdale, W. J.; Bartlett, R. J. *Int. J. Quantum Chem. Symp.* **1992**, *26*, 879.
- (10) Nicolaidis, A.; Rauk, A.; Glukhovtsev, M. N.; Radom, L. *J. Phys. Chem.* **1996**, *100*, 17460.
- (11) Wagman, D. D.; Evans, W. H.; Parker, V. B.; Schumm, R. H.; Halow, I.; Bailey, S. M.; Churney, K. L.; Nuttall, R. L. *J. Phys. Chem. Ref. Data* **1982**, *17* (Suppl. 2).
- (12) (a) Mayer, P. M.; Parkinson, C. J.; Smith, D. M.; Radom, L. *J. Chem. Phys.* **1998**, *108*, 604. (b) We note that the extent of spin-contamination is significantly reduced (compared with UHF) at the quadratic configuration interaction level, which is part of the G2 procedure. For example, the $\langle S^2 \rangle$ value for $\cdot\text{CH}_2\text{CN}$ is 0.898 at UHF/6-311G(d,p) but is reduced to 0.760 at UQCISD/6-311G(d,p).
- (13) We found virtually no change in the geometries of the HCF^- and HCCN^- radical anions on going from the 6-31G(d) to 6-31+G(d) basis sets at the MP2(full) level of theory (Table S3). Accordingly, the G2 $\Delta_{\text{acid}}H^\circ$ values for $\cdot\text{CH}_2\text{F}$ and $\cdot\text{CH}_2\text{CN}$ are essentially the same using the two geometries (Table S3).
- (14) Lias, S. G.; Bartmess, J. E.; Liebman, J. F.; Holmes, J. L.; Levin, R. D.; Mallard, W. G. *J. Phys. Chem. Ref. Data* **1988**, *17* (Suppl. 1).
- (15) (a) Boyd, S. L.; Boyd, R. J.; Bessonette, P. W.; Kerdraon, D. I.; Aucoin, N. T. *J. Am. Chem. Soc.* **1995**, *117*, 8816. (b) Boyd, S. L.; Boyd, R. J. *J. Am. Chem. Soc.* **1997**, *119*, 4214.
- (16) Mayer, P. M.; Glukhovtsev, M. N.; Gauld, J. W.; Radom, L. *J. Am. Chem. Soc.* **1997**, *119*, 12889.
- (17) Radom, L. *Prog. Theor. Org. Chem.* **1981**, *3*, 1.
- (18) (a) Hawari, J. A.; Kanabus-Kaminska, J. M.; Wayner, D. D. M.; Griller, D. In *Substituent Effects in Radical Chemistry*; Viehe, H. G., Janousek, Z., Merenyi, R., Eds.; D. Reidel: Dordrecht, 1986; p 91. (b) Leroy, G.; Peeters, D.; Sana, M.; Wilante, C. In *Substituent Effects in Radical Chemistry*; Viehe, H. G., Janousek, Z., Merenyi, R., Eds.; D. Reidel: Dordrecht, 1986; p 1. (c) Pasto, D. J. *J. Am. Chem. Soc.* **1988**, *110*, 8164. (d) Bordwell, F. G.; Lynch, T.-Y. *J. Am. Chem. Soc.* **1989**, *111*,

7558. (e) Lehd, M.; Jensen, F. *J. Org. Chem.* **1991**, *56*, 884. (f) Bordwell, F. G.; Zhang, X.-M.; Alnajjar, M. S. *J. Am. Chem. Soc.* **1992**, *114*, 7623.

(19) (a) Jorgensen, W. L.; Briggs, J. M. *J. Am. Chem. Soc.* **1989**, *111*, 4190. (b) El-Nahas, A. M.; Schleyer, P. v. R. *J. Comput. Chem.* **1994**, *15*, 596.

(20) (a) Matimba, H. E. K.; Crabbendam, A. M.; Ingemann, S.; Nibbering, N. M. M. *Int. J. Mass Spectrom. Ion Processes* **1992**, *114*, 85. (b) Born, M.; Ingemann, S.; Nibbering, N. M. M. *J. Am. Chem. Soc.* **1994**, *116*, 7210.

(21) (a) Griller, D.; Lossing, F. P. *J. Am. Chem. Soc.* **1981**, *103*, 1586. (b) Ruscic, B.; Berkowitz, J. *J. Phys. Chem.* **1993**, *97*, 11451. (c) Dóbé, S.; Bérces, T.; Turányi, T.; Márta, F.; Grossdorf, J.; Temps, F.; Wagner, H. G. *J. Phys. Chem.* **1996**, *100*, 19864. (d) Good, D. A.; Francisco, J. S. *Chem. Phys. Lett.* **1997**, *266*, 512. (e) Holmes, J. L.; Lossing, F. P. *Int. J. Mass*

Spectrom. Ion Processes **1984**, *58*, 113. (f) Ruscic, B.; Berkowitz, J. *J. Chem. Phys.* **1992**, *97*, 1818. (g) Espinosa-Garcia, J. *Chem. Phys. Lett.* **1996**, *250*, 71. (h) Pickard, J. M.; Rogers, A. S. *Int. J. Chem. Kinet.* **1983**, *15*, 569. (i) Seetula, J. A. *J. Chem. Soc., Faraday Trans.* **1996**, *92*, 3069. (j) Holmes, J. L.; Lossing, F. P. *J. Am. Chem. Soc.* **1988**, *110*, 7343. (k) Rossi, M.; Golden, D. M. *Int. J. Chem. Kinet.* **1979**, *11*, 715. (l) Holmes, J. L.; Lossing, F. P.; Terlouw, J. K. *J. Am. Chem. Soc.* **1986**, *108*, 1086. (m) Holmes, J. L.; Mayer, P. M. *J. Phys. Chem.* **1995**, *99*, 1366.

(22) (a) Ma, Z.-X.; Liao, C.-L.; Ng, C. Y.; Ma, N. L.; Li, W.-K. *J. Chem. Phys.* **1993**, *99*, 6470. (b) Moran, S.; Ellis, H. B.; DeFrees, D. J.; McLean, A. D.; Ellison, G. B. *J. Am. Chem. Soc.* **1987**, *109*, 5996. (c) Moran, S.; Ellis, H. B.; DeFrees, D. J.; McLean, A. D.; Paulson, S. E.; Ellison, G. B. *J. Am. Chem. Soc.* **1987**, *109*, 6004.